Journal of Membrane Science 379 (2011) 233–238

Contents lists available at ScienceDirect

Journal of Membrane Science

journal homepage: www.elsevier.com/locate/memsci

Effects of three natural organic matter types on cellulose acetate butyrate microfiltration membrane fouling

Masatoshi Hashino[a,b], Keisuke Hirami[a], Takeshi Katagiri[a], Noboru Kubota[b], Yoshikage Ohmukai[a], Toru Ishigami[a], Tatsuo Maruyama[a], Hideto Matsuyama[a,*]

[a] Center for Membrane and Film Technology, Department of Chemical Science and Engineering, Kobe University, 1-1 Rokkodai, Nada, Kobe 657-8501, Japan
[b] Microza & Water Processing Division, Asahi-Kasei Chemicals Co. Ltd, Fuji, Shizuoka 416-8501, Japan

ARTICLE INFO

Article history:
Received 14 February 2011
Received in revised form 26 April 2011
Accepted 28 May 2011
Available online 6 June 2011

Keywords:
Membrane fouling
Natural organic matter
Quartz crystal microbalance
Hollow fiber membrane
Backwashing

ABSTRACT

This study aimed to clarify the effect of interactions between membranes and natural organic matter (NOM), which is considered to be the major membrane foulant in wastewater treatment processes. Sodium alginate (SA), humic acid (HA) and bovine serum albumin (BSA) were used as NOM models. Hollow fiber membranes were prepared using cellulose acetate butyrate polymer (CAB). Filtration experiments were carried out using SA, HA and BSA solutions and the membrane fouling behavior was examined. NOM adsorption on CAB membranes was measured by quartz crystal microbalance with dissipation (QCM-D), where NOM solutions were flowed across CAB spin-coated quartz crystal sensors and adsorbed. SA showed more severe permeate flux decline during the early stage of filtration and lower recovery of permeate flux after backwashing compared with HA. The severe flux decline for SA was due to pore-plugging and cake formation with high molecular weight components. The BSA solution, with no high molecular components, showed a gradual permeate flux decline and resulted in lower permeate flux after 240 min filtration compared with HA. The gradual permeate flux decline with the BSA solution was due to ready adsorption of BSA on the CAB membrane.

1. Introduction

Membrane technologies such as microfiltration (MF) and ultrafiltration (UF) are attractive for drinking water and wastewater treatment due to complete particle removal, including microorganisms such as protozoa (Giardia and Cryptosporidium) [1,2]. The obstacle to more widespread use of membrane technology is membrane fouling, which decreases permeability, resulting in conservative design flux [3]. Some organic and inorganic materials in the feed water that accumulate on the membrane surface or within the pores during filtration are removed by periodical physical cleaning, such as backwashing and air-bubbling. Membranes for which performances cannot be recovered by physical cleaning only are treated by chemical cleaning using an oxidizer, alkali, and acid. Thus, membrane fouling causes increased operating costs, including energy and chemical consumption, and shortened membrane life, which limits widespread use of membrane technology [4,5].

Many studies have been carried out on characterizing membrane foulants and membrane fouling mechanisms. With respect to characterization of membrane foulants, natural organic matters (NOM), which are products of chemical and biological degradation of plant and animal residues [6], are considered the major membrane foulants [7]. In previous studies, it was reported that both hydrophobic NOM components, such as humic substances [8–11], and hydrophilic NOM components, such as polysaccharide- and protein-like substances [12–16], contributed to membrane fouling. It was also reported that synergy between hydrophobic and hydrophilic NOM [17] or NOM and inorganic matters [18,19] affected membrane fouling. With respect to membrane fouling mechanisms, Yuan et al. reported that large particles of humic acid played an important role in initial fouling during microfiltration of humic acid solutions [20]. Yamamura et al. conducted a pilot-scale microfiltration test on surface water and reported that membrane foulants changed from relatively large particles to small particles during filtration [21].

For better understanding and control of membrane fouling, more information about the effect of the interactions between NOMs and membranes on membrane fouling is required. Shäfer et al. examined the effect of colloid size on membrane fouling and found that the colloids with sizes closest to the membrane pore size caused the greatest flux decline [22]. A number of researchers examined adsorption of NOM on membranes [23–25]. Jucker et al. [23] and Jones et al. [24] reported that the adsorption of NOMs such as humic acid, fulvic acid and protein on the membrane surface was influenced by solution chemistry such as pH, ionic strength and presence of calcium. Quartz crystal microbalance with dissipation

* Corresponding author. Tel.: +81 78 803 6180; fax: +81 78 803 6180.
E-mail address: matuyama@kobe-u.ac.jp (H. Matsuyama).

0376-7388/$ – see front matter © 2011 Elsevier B.V. All rights reserved.
doi:10.1016/j.memsci.2011.05.068

(QCM-D) monitoring is an attractive method for examining NOM adsorption on organic and inorganic surfaces [26–28]. When an NOM solution is passed through the flow chamber equipped with a polymer (e.g. poly(methyl methacrylate) [26] or polyethersulfone [27]) spin-coated quartz crystal sensor, the resonant frequency of the quartz crystal sensor decreases with adsorbed mass and information about adsorption extent and adlayer properties can be obtained. The QCM-D method is expected to be a powerful tool in clarifying the effect of NOM adsorption on membrane fouling.

The objective of this study was to elucidate the effect of interactions between membranes and NOMs on membrane fouling to improve understanding and control of membrane fouling. CAB polymer was used as a membrane material due to its good resistance to fouling, chemical tolerance and easiness in controlling of membrane structure [29]. We prepared hollow fiber membranes from CAB polymer via thermally induced phase separation and then compared membrane fouling by sodium alginate and BSA as models of hydrophilic NOMs with that by humic acid as a model of a hydrophobic NOM. Differences in membrane fouling behaviors for three types of NOMs were examined from the view point of the interaction between the CAB membrane and NOMs using QCM-D measurements.

2. Experimental

2.1. Materials

Cellulose acetate butyrate (CAB, Mw = 65,000, Daicel Chemical Industries, Japan) was used as a membrane material. The substitution degrees of acetyl and butyryl groups were 2.04 and 0.71, respectively. Triethylene glycol (TEG, Wako Pure Chemical Industries, Japan) was used as a diluent for membrane preparation via thermally induced phase separation. The sodium alginate filtration solution was prepared by mixing sodium alginate (Aldrich Chemical Co., Milwaukee, WI) with sodium bicarbonate (Wako Pure Chemical Industries) as a buffer. The humic acid (Aldrich Chemical Co.) solution was also prepared with sodium bicarbonate. The bovine serum albumin (BSA) solution was prepared by mixing BSA with a sodium dihydrogen phosphate/disodium hydrogen phosphate buffer solution at pH 7 (all reagents from Wako Pure Chemical Industries). All chemicals were used without further purification.

2.2. Preparation of hollow fiber CAB membrane

Hollow fiber membranes were prepared using a batch-type extruder via thermally induced phase separation (TIPS) under the preparation conditions shown in Table 1. CAB polymer and TEG were placed into a vessel equipped with a stirrer and heated to 443 K. The mixture was then blended for 1 h and held for 2 h to remove air bubbles from the polymer solution. The homogeneous polymer solution was fed to a spinneret with a gear pump using N_2 gas pressure. The spinneret consisted of an inner tube with a diameter of 0.83 mm and an outer tube with a diameter of 1.58 mm. The hollow fiber was extruded from the spinneret with TEG as an inner coagulant and was introduced into a water bath at 323 K, where phase separation proceeded and the porous structure was solidified. The hollow fiber was wound at a take-up speed of 0.21–0.26 m/s. Finally, residual TEG in the membrane was extracted by water.

Table 1
Preparation conditions for the hollow fiber membranes.

Spinneret size (mm)	1.58/0.83 (outer/inner diameter)
Polymer solution	CAB (25 wt.%)-TEG
Solution temperature (K)	443
Polymer solution flow rate (m/s)	0.17–0.19
Inner coagulant	TEG
Inner coagulant flow rate (m/s)	0.17–0.19
Inner coagulant temperature (K)	298
Take-up speed (m/s)	0.21–0.26
Air gap (mm)	0
Bath composition	Water
Bath temperature (K)	323

2.3. SEM observation

The hollow fiber membrane was freeze–dried (FD-1000 freeze dryer, EYELA, Japan). The dry hollow fiber membrane was immersed into liquid nitrogen, broken, and treated by Au/Pd sputtering. Scanning electron microscope (SEM, Hitachi Co., JSM-5610LVS, Japan) images of the outer and inner surfaces of the hollow fiber membrane were measured at an accelerating voltage of 15 kV.

2.4. Filtration experiments

A diagram of the filtration-backwashing experiments with the single hollow fiber module is shown in Fig. 1. Feed solution was pumped into a module packed with a single hollow fiber of length of about 110 mm (effective membrane area = 3.5×10^{-4} m^2). Cross-flow filtration was carried out from the outer surface to the inner surface of the hollow fiber at a transmembrane pressure of 50 kPa and a cross-flow rate of 0.04 m/s. For each filtration experiment, deionized (DI) water was initially permeated and the pure water permeability J_0, was measured. Feed solution, consisting of 50 mg/L sodium alginate and 0.5 mmol/L sodium bicarbonate as a buffer solution (pH 8), was filtered and the permeability of the sodium alginate solution, J, was measured. After filtration for 1 h, backwashing with DI water was carried out for 1 min at a pressure of 100 kPa. The filtration-backwashing cycle was repeated four times. During filtration of sodium alginate, concentrations of sodium alginate in the feed and permeate were measured using a total organic carbon (TOC) meter (Shimadzu Co., TOC-V, Japan). Rejection of sodium alginate was calculated as:

$$\text{Rejection}\,(\%) = \frac{C_0 - C}{C_0} \times 100 \quad (1)$$

where C_0 and C are the TOC in feed and permeate, respectively.

Filtration experiments for solutions containing 50 mg/L humic acid and BSA were carried out in a same way on feed solutions prepared as described in Section 2.1. The rejections of humic acid and BSA were calculated according to Eq. (1) by measuring the absorbance at wavelengths of 254 nm and 280 nm, respectively, with a spectrometer (Hitachi Co., U-2000, Japan).

2.5. Apparent molecular weight distribution measurement

Apparent molecular weight distributions for the solutions of sodium alginate, humic acid and BSA solutions were measured by the membrane fractionation method using ultrafiltration and microfiltration membranes [10,20,30]. 50 mg/L of sodium alginate, humic acid and BSA solutions prepared in the manner described in Section 2.1 were used as feeds. Three kinds of ultrafiltration membranes used were Amicon® ultra with nominal molecular weight limits (NMWLs) of 30, 50 and 100 kDa (Millipore). Microfiltration membranes with pore sizes of 0.1 and 0.45 μm were also used (Durapore® membrane filter, Millipore). The concentrations in the feed and permeate for sodium alginate, humic acid and BSA were measured as described above and the apparent molecular weight distributions were calculated from the resultant rejections using the ultrafiltration and microfiltration membranes.

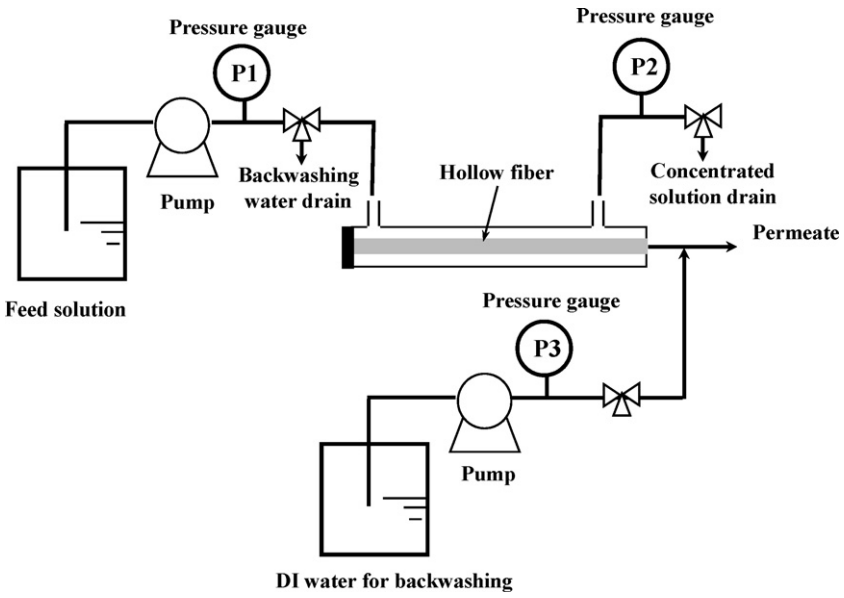

Fig. 1. Diagram of filtration-backwashing experiments using a single hollow fiber module.

2.6. Measurement of NOM adsorption on CAB film

QCM-D was used to measure the adsorbed amount of NOMs on CAB films. A 0.5 wt.% CAB solution in tetrahydrofuran was spin-coated onto a piezoelectric quartz crystal sensor with a fundamental resonant frequency of 4.95 MHz and diameter 14 mm (Q-Sense, QSX 301, Sweden) pre-cleaned using a UV/Ozone cleaner (BioForce Nanosciences, Pro Cleaner 110) and dried on a hotplate (IKA GmbH, C-MAG HP4) at 353 K for 30 min.

QCM-D measurements were conducted using a QCM-D E1 (Q-Sense) with flow chamber, equipped with the CAB-coated quartz crystal sensor. The buffer solutions used in the preparation of each

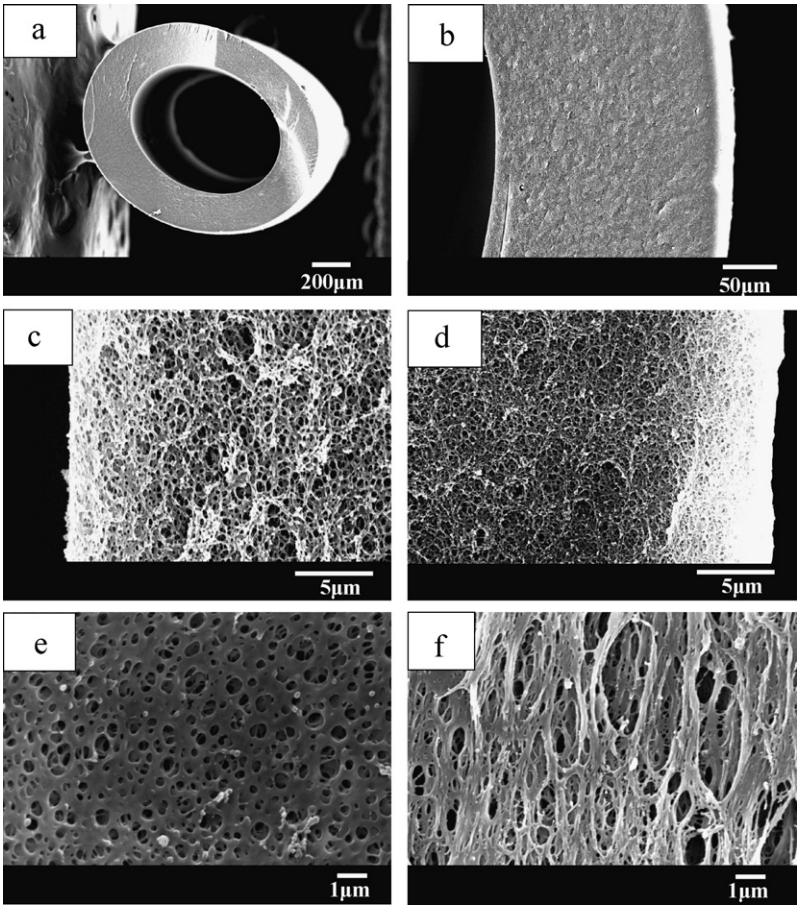

Fig. 2. SEM images of the hollow fiber membrane prepared by the TIPS method: (a) whole cross section; (b) enlarged cross section; (c) cross-section near the inner surface; (d) cross-section near the outer surface; (e) inner surface; (f) outer surface.

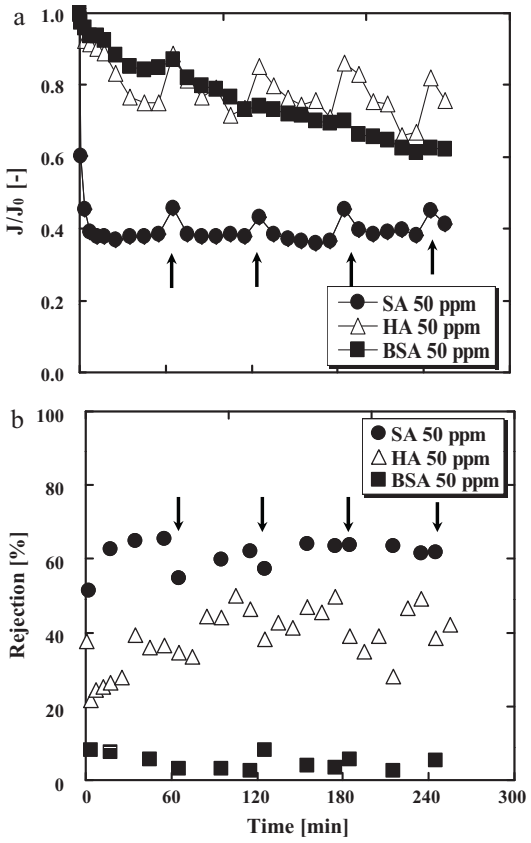

Fig. 3. Relative permeability (a) and rejection (b) as a function of filtration time for 50 mg/L sodium alginate (SA), humic acid (HA) and BSA solutions. Arrows in the figure show the backwashing process.

NOM solution were supplied into the flow chamber at a flow rate of 40 μl/min for more than 10 min to stabilize the sensor. 50 mg/L sodium alginate, humic acid and BSA solutions (Section 2.1) were then supplied for 30 min. The change in frequency (Δf) is correlated to the adsorbed amount per unit surface of NOMs on the sensor (Δm) by the Sauerbrey equation [31]:

$$\Delta m = \frac{-C \cdot \Delta f}{n} \quad (2)$$

where C is the mass sensitivity constant (= 17.7 ng/cm^2/Hz at f = 4.95 MHz) and n is the overtone number (n = 7 in this study).

3. Results and discussion

3.1. Hollow fiber membrane

SEM images of the outer and inner surfaces for the membrane prepared via TIPS are shown in Fig. 2. Both cross sections and surface structures are shown in this figure. As shown in Fig. 2(e) and (f), the outer and inner surfaces of the membrane were porous, with submicron pore sizes. The air gap during membrane preparation was zero and triethylene glycol (diluent for the CAB polymer) was used as an inner coagulant. Thus, diluent evaporation from the outer and inner surfaces was prevented, which led to porous structures at both surfaces. The pure water permeability of the membrane was about 300 L/(m^2 bar h).

3.2. Filtration experiments for NOM solutions

The results of filtration experiments for 50 mg/L sodium alginate, humic acid and BSA solutions are shown in Fig. 3. The membrane fouling behaviors differed between the three kinds of NOM. The relative permeability of sodium alginate solution J/J_0 decreased rapidly during the early stage of the filtration and reached a minimum of 0.4 after 240 min. For the humic acid solution, the initial decline of relative permeability was also rapid up to 60 min, while the relative permeability after 240 min reached a maximum of about 0.7, higher than that of sodium alginate. In both cases, permeability decreased rapidly during the initial filtration and reached steady values. This indicates that membrane fouling may proceed by pore plugging during the early stage of filtration, followed by cake layer formation, as reported by Ye et al. [32]. On the other hand, for the BSA solution, the relative permeability decreased gradually with filtration time and reached 0.6 after 240 min, which was lower than that of the humic acid solution. Rejections of sodium alginate, humic acid and BSA by the CAB membrane are shown in Fig. 3(b). The rejections of sodium alginate increased rapidly over a short filtration time and reached about 65%. The rejections of humic acid were lower than those of sodium alginate. The rejections for BSA were very low (less than 10%) during filtration experiments.

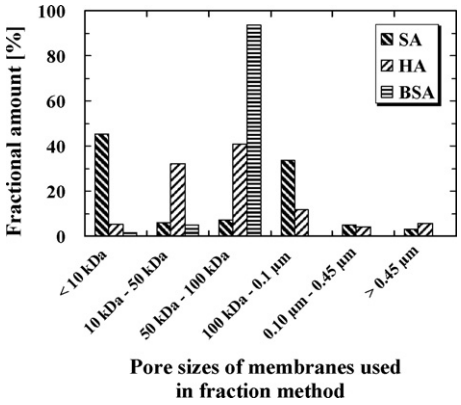

Fig. 4. Apparent molecular weight distributions for sodium alginate (SA), humic acid (HA) and BSA solutions.

The differences between the rejections among the three types of NOM were further examined by measuring the apparent molecular weight distributions for each. Fig. 4 shows the apparent molecular weight distributions for sodium alginate, humic acid and BSA measured by the membrane fraction method. For both sodium alginate and humic acid, there were components above 0.1 μm, which were close to the pore size of the outer membrane surface, as shown in Fig. 2(e), and may have caused pore-plugging, resulting in the rapid flux decline during the early stages of filtration. These results are in agreement with the result reported by Yuan et al. that the initial membrane fouling with humic acid in microfiltration was significantly influenced by the large molecular weight components [20]. The fractional amount of high molecular weight components exceeding 0.1 μm was about 8% for both sodium alginate and humic acid, as shown in Fig. 4. This was much lower than the initial rejections of sodium alginate (50%) and humic acid (20%) shown in Fig. 3(b). Therefore, it is concluded that the pore size on the membrane outer surface was reduced through pore-plugging by components larger than 0.1 μm and components of size 100 kDa to 0.1 μm were subsequently retained by the membrane during initial filtration. The fractional amount of 100 kDa to 0.1 μm for sodium alginate (33%) was higher than that for humic acid (12%). This explains why the relative permeability and rejection of sodium alginate were lower and higher, respectively, than those of humic acid, as shown in Fig. 3. On the other hand, BSA had a main molecular weight range of 50–100 kDa, corresponding to the molecular weight of BSA (66–68 kDa [33]) and had no components with molecular weight exceeding 100 kDa. Thus, the size

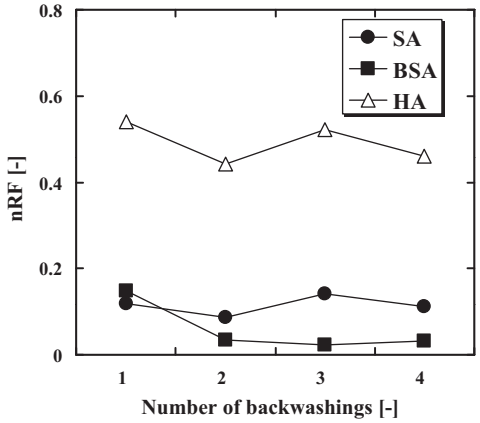

Fig. 5. *nRF* for sodium alginate (SA), humic acid (HA) and BSA solutions.

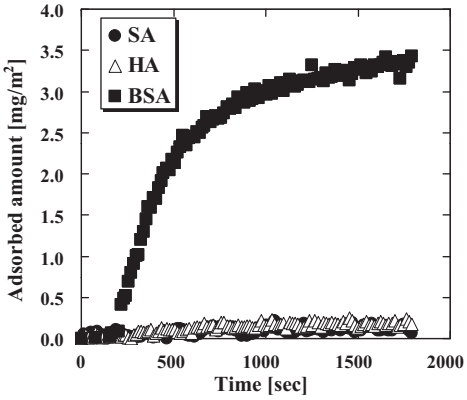

Fig. 6. Amounts of sodium alginate (SA), humic acid (HA) and BSA adsorbed on CAB spin-coated quartz crystal sensors as a function of time.

of BSA was much smaller than the surface pore size, as shown in Fig. 2(e), and BSA may therefore adsorb on the pore surface, leading to a gradual and prolonged relative permeability decline. From these results, it was found that the high molecular weight components with sizes close to those of the membrane outer pores caused the rapid flux decline within a short filtration time and steric interactions between NOM and membrane played an important role in the initial membrane fouling.

The difference between the relative permeabilities of sodium alginate and humic acid should be also considered from the viewpoint of the intermolecular interaction of NOM–NOM in the cake layer. Sodium alginate, which has many hydroxyl groups in its molecular structure, shows strong intermolecular interaction by hydrogen bonding. On the other hand, humic acid, in which carboxyl groups were dissociated into ions at pH of 8 in this study, shows weak intermolecular interaction by electrostatic repulsion. Blake et al. proposed that cross-flow filtration was affected by the inter-particle force on the membrane surface as well as the forces applied to the particles by convection and tangential flow [34]. Also, in this study, the effect of cross-flow may be constrained by stronger intermolecular interactions between each sodium alginate, leading to the formation of a thicker cake layer, followed by the severe permeate flux decline shown in Fig. 3.

A normalized reversible flux, *nRF*, was calculated using the following equation:

$$nRF = \frac{J_a - J_b}{J_0 - J_b} \quad (3)$$

where J_a is the permeability after backwashing and J_b is the permeability before backwashing. *nRF* describes the proportion of reversible fouling that can be removed by backwashing. The *nRF* calculated based on the data in Fig. 3 is shown in Fig. 5 for the three types of NOMs. Humic acid showed a higher *nRF* (about 0.5) than sodium alginate (about 0.1) and BSA (about 0.05), leading to a higher permeate flux in prolonged filtration. The difference in *nRF* between the three types of NOM cannot be explained simply by the difference of molecular size. To understand the difference in *nRF* between sodium alginate and humic acid, the interactions between the NOM–CAB membrane and NOM–NOM in the cake layer should be considered. The fouling mechanism for both NOMs was pore-plugging, followed by cake layer formation, as mentioned above. Therefore, the hydraulic flow during backwashing is needed to overcome the intermolecular interaction between NOMs in the cake layer as well as the interaction force between NOM and membrane surface. Because hydroxyl groups are the predominant functional groups of sodium alginate and carboxyl groups is predominant in humic acid, the interaction force between NOM–CAB membrane and NOM–NOM for sodium alginate were stronger than those of humic acid, due to hydrogen bonding. Thus, *nRF* for sodium alginate was lower than that of humic acid. Although BSA had no high molecular weight components, the BSA solution showed a lower *nRF* compared with sodium alginate and humic acid solutions. Because the size of BSA is much smaller than the pore sizes in the CAB membrane, BSA can penetrate deeper into the membrane and be adsorbed. Therefore, BSA cannot be removed effectively by back-washing, resulting in a lower *nRF*.

3.3. QCM measurements

Fig. 6 shows the amounts of sodium alginate, humic acid and BSA adsorbed on the CAB-coated quartz crystal sensor. The amount of BSA adsorbed was about 3.3 mg/m^2 and was much higher than those of sodium alginate and humic acid (about 0.2 mg/m^2). These results are consistent with those reported by Contreras et al. that BSA adsorbed on a silica-coated quartz crystal sensor but humic acid and sodium alginate did not adsorb due to electrostatic repulsion between these negatively charged molecules and the negatively charged silica surface [28]. The CAB film in this study was also negatively charged [35] and so electrostatic repulsion between the negatively charged NOMs (sodium alginate and humic acid) and CAB prevented their adsorption on the CAB film. Because the isoelectric point of BSA is 4.8 [33], BSA also has a negative charge in the feed solution (pH 7). However, BSA has a lower charge density than sodium alginate or humic acid, leading to smaller electrostatic repulsion [28]. It has also been pointed out that adsorption of protein on polymer surfaces may be affected by hydrophobic interactions as well as electrostatic repulsion [27]. In this study, hydrophobic interaction between BSA and CAB might also overcome the electrostatic repulsion, leading to the higher amount adsorbed. Although more BSA was found to be adsorbed on the CAB film by the QCM-D experiments, the initial permeate flux decline for the BSA solution was lower than those of sodium alginate and humic acid, as shown in Fig. 3(a). This result indicates that the initial permeate flux declines seen in the presence of the NOM solutions were due to pore-plugging, based on steric interaction between NOMs and membranes rather than physicochemical interactions. On the other hand, the BSA solution had no high molecular weight components, as shown in Fig. 4, while the permeate flux of the BSA solution after 240 min was at a lower level than that of the humic acid solution having high molecular weight components, as shown in Fig. 3(a). This result also indicates that the prolonged permeate flux decline in the case of BSA was due to pore-plugging based on a physicochemical interaction between NOMs and membranes as well as steric interaction.

4. Conclusions

The influence of NOM type on fouling of CAB membranes was examined using sodium alginate, humic acid and BSA solutions. The membrane fouling behaviors of these NOMs differed, depending on the interaction between the NOMs and the CAB membrane. The sodium alginate solution showed more severe flux decline than humic acid and BSA, due to pore-plugging and subsequent cake layer formation with high molecular weight components with sizes exceeding 0.1 μm. On the other hand, the BSA solution, which contained no high molecular weight components, showed lower initial membrane fouling than sodium alginate and humic acid but the permeate flux after 240 min filtration for the BSA solution was lower than that of humic acid. QCM-D measurements showed much greater amounts of BSA adsorbed on a CAB film than sodium alginate or humic acid, indicating that adsorption of BSA on the pore surface leads to gradual and prolonged membrane fouling.

Acknowledgment

This work was financially supported by Special Coordination Funds for Promoting Science and Technology from the Creation of Innovation Centers for Advanced Interdisciplinary Research Areas (Innovative Bioproduction Kobe), MEXT, Japan.

References

[1] J.G. Jacangelo, S.S. Adham, J.-M. Laîné, Mechanism of cryptosporidium, Giardia, and MS2 virus removal by MF and UF, J. AWWA 87 (1995) 107.
[2] S.S. Adham, J.G. Jacangelo, J.-M. Laîné, Characteristics and costs of MF and UF plants, J. AWWA 88 (1996) 22.
[3] M.F.A. Goosen, S.S. Sablani, H. Al-Hinai, S. Al-Obeidani, R. Al-Belushi, D. Jackson, Fouling of reverse osmosis and ultrafiltration membranes: a critical review, Sep. Sci. Technol. 39 (2004) 2261.
[4] M.R. Wiesner, S. Chellam, The promise of membrane technology, Environ. Sci. Technol. 33 (1999) 360A.
[5] M. Grander, B. Jefferson, S. Judd, Aerobic MBRs for domestic wastewater treatment: a review with cost considerations, Sep. Purif. Technol. 18 (2000) 119.
[6] N. Her, G. Amy, D. Foss, J. Cho, Y. Toon, P. Kosenka, Optimization of method for detecting and characterizing NOM by HPLC-size exclusion chromatography with UV and on-line DOC detection, Environ. Sci. Technol. 36 (2002) 1069.
[7] K.J. Howe, A. Marwah, K.P. Chiu, S.S. Adham, Effect of coagulation on the size of MF and UF membrane foulants, Environ. Sci. Technol. 40 (2006) 7908.
[8] K. Ruohomäki, P. Väisänen, S. Metsämuuronen, M. Kulovaara, M. Nyström, Characterization and removal of humic substances in ultra- and nanofiltration, Desalination 118 (1998) 273.
[9] W. Yuan, A.L. Zydney, Effects of solution environment on humic acid fouling during microfiltration, Desalination 122 (1999) 63.
[10] W. Yuan, A.L. Zydney, Humic acid fouling during ultrafiltration, Environ. Sci. Technol. 34 (2000) 5043.
[11] K. Katsoufidou, S.G. Yiantsios, A.J. Karabelas, A study of ultrafiltration membrane fouling by humic acids and flux recovery by backwashing: experiments and modeling, J. Membr. Sci. 266 (2005) 40.
[12] T. Carroll, S. King, S.R. Gray, B.A. Bolto, N.A. Booker, The fouling of microfiltration membranes by NOM after coagulation treatment, Water Res. 34 (2000) 2861.
[13] L. Fan, J.L. Harris, F.A. Roddick, N.A. Booker, Influence of the characteristics of natural organic matter on the fouling of microfiltration membranes, Water Res. 35 (2001) 4455.
[14] K. Kimura, Y. Hane, Y. Watanabe, G. Amy, N. Ohkuma, Irreversible membrane fouling during ultrafiltration of surface water, Water Res. 38 (2004) 3431.
[15] N. Lee, G. Amy, J.-P. Croûe, H. Buisson, Identification and understanding of fouling in low-pressure membrane (MF/UF) filtration by natural organic matter (NOM), Water Res. 38 (2004) 4511.
[16] N. Lee, G. Amy, J.-P. Croûe, Low-pressure membrane (MF/UF) fouling associated with allochthonous versus autochthonous natural organic matter, Water Res. 40 (2006) 2357.
[17] D. Jermann, W. Pronk, S. Meylan, M. Boller, Interplay of differential NOM fouling mechanisms during ultrafiltration for drinking water production, Water Res. 41 (2007) 1713.
[18] M. Zhang, C. Li, M.M. Benjamin, Y. Chang, Fouling and natural organic matter removal in adsorbent/membrane systems for drinking water treatment, Environ. Sci. Technol. 37 (2003) 1663.
[19] D. Jermann, W. Pronk, R. Kagi, M. Halbeisen, M. Boller, Influence interaction between NOM and particles of UF fouling mechanisms, Water Res. 42 (2008) 3870.
[20] W. Yuan, A.L. Zydney, Humic acid fouling during microfiltration, J. Membr. Sci. 157 (1999) 1.
[21] H. Yamamura, S. Chae, K. Kimura, Y. Watanabe, Transition in fouling mechanism in microfiltration of a surface water, Water Res. 41 (2007) 3812.
[22] A.I. Schäfer, U. Schwicker, M.M. Fischer, A.G. Fane, T.D. Waite, Microfiltration of colloids and natural organic matter, J. Membr. Sci. 171 (2000) 151.
[23] C. Jucker, M.M. Clark, Adsorption of aquatic humic substances on hydrophobic ultrafiltration membranes, J. Membr. Sci. 97 (1994) 37.
[24] K.L. Jones, C.R. O'Melia, Protein and humic acid adsorption onto hydrophilic membrane surfaces, effects of pH and ionic strength, J. Membr. Sci. 165 (2000) 31.
[25] H. Susanto, M. Ulbricht, Influence of ultrafiltration membrane characteristics on adsorptive fouling with dextrans, J. Membr. Sci. 266 (2005) 132.
[26] C. Liu, B.J. Meenan, Effect of air plasma processing on the adsorption behavior of bovine serum albumin on spin-coated PMMA surfaces, J. Bionic Eng. 5 (2008) 204.
[27] J.T. Kim, N. Weber, G.H. Shin, Q. Huang, S.X. Liu, The study of β-lactoglobulin adsorption on polyethersulfone thin film surface using QCM-D and AFM, J. Food Sci. 72 (2007) 214.
[28] A.E. Contreras, A. Kim, Q. Li, Combined fouling of nanofiltration membranes: mechanisms and effect of organic matter, J. Membr. Sci. 327 (2009) 87.
[29] X.Y. Fu, T. Sotani, H. Matsuyama, Effect of membrane preparation method on the outer surface roughness of cellulose acetate butyrate hollow fiber membrane, Desalination 233 (2008) 10.
[30] M. Taniguchi, J.E. Kilduff, G. Belfort, Modes of natural organic matter fouling during ultrafiltration, Environ. Sci. Technol. 37 (2003) 1676.
[31] G. Sauerbrey, The use of quartz oscillators for weighing thin layers and for microweighing, Z. Phys. 155 (1959) 206.
[32] Y. Ye, P. Le Clech, V. Chen, A.G. Fane, B. Jefferson, Fouling mechanisms of alginate solutions as model extracellular polymeric substances, Desalination 175 (2005) 7–20.
[33] D.A. Musale, S.S. Kulkarni, Relative rates of protein transmission through poly(acrylonitrile) based ultrafiltration membranes, J. Membr. Sci. 136 (1997) 13.
[34] N.J. Blake, I.W. Cumming, M. Streat, Prediction of steady state crossflow filtration using a force balance model, J. Membr. Sci. 68 (1992) 205.
[35] X. Fu, T. Maruyama, T. Sotani, H. Matsuyama, Effect of surface morphology on membrane fouling by humic acid with the use of cellulose acetate butyrate hollow fiber membranes, J. Membr. Sci. 320 (2008) 483.